Electronic Supplementary Material (ESI) for Journal of Materials Chemistry A.

Mesoporous N-doped Carbon-Coated CoSe Nanocrystals Encapsulated in S-Doped Carbon Nanosheets as Advanced Anode with Ultrathin Solid Electrolyte Interphase for High-Performance Sodium-Ion Half/Full Batteries

Zhonghui Sun,[a] Zhenyi Gu,[b] Wenjun Shi,[a] Zhongbo Sun,[c] Shiyu Gan,[a] Longbin Xu,[a] Haojie Liang,[b] Yingming Ma,[a] Dongyang Qu,[a] Lijie Zhong,[a] Dongxue Han,*[a] Xing-Long Wu,[b] and Li Niu*[a]

[a.] *Guangzhou Key Laboratory of Sensing Materials & Devices, c/o Center for Advanced Analytical Science, School of Chemistry and Chemical Engineering, Guangzhou University, Guangzhou, Guangdong 510006, China*
E-mail: lniu@gzhu.edu.cn; dxhan@gzhu.edu.cn;
[b.] *MOE Key Laboratory for UV Light-Emitting Materials and Technology, Northeast Normal University, Changchun, Jilin 130024, P. R. China.*
[c.] *Department of Control Engineering, Changchun University of Technology, Changchun, Jilin 130012, China*
Z. H. Sun and Z. Y. Gu contributed equally.

1. Experimental Section

Chemicals: All the chemical reagents were analytical grade and used without further purification.

1.1 Synthesis of Co-MOF nanosheets and Co-NTAC nanorods.

First, 0.996 g of $Co(CH_3COO)_2{\cdot}4H_2O$ and 3.043 g of p-toluenesulfonic acid were dispersed in 30 mL deionized water. Then, 2 mL of the concentrated ammonia solution (28%) was added into the above solution under continuous stirring for 2 h. Finally, the obtained precipitate was washed with deionized water and dried overnight.

The precursor Co-NTAC nanorods were prepared as follows. First, 0.77 g of $CoCl_2{\cdot}6H_2O$ and 0.6 g of nitrilotriacetic acid were added into a mixture of 40 mL of 2-propanol and deionized water. Then the obtained mixture was transferred into a 50 mL stainless steel Teflon-lined autoclave and kept at 180 °C for 6 h. After reaction, the Co-NTAC was collected via centrifugation and washed by deionized water and dried overnight.

1.2 Preparation of core-shell Co-MOF@MPDA (Co-NTAC@MPDA) composites.

The as-obtained Co-MOF nanosheets (Co-NTAC nanorods) was dispersed in a mixture of ethanol and deionized water (in volume rate 1:1). Then, 0.075 g of Pluronic F127, 0.25 mL of trimethylbenzene and 0.075 g of dopamine were added subsequently under stirring. After that, 0.2 mL of concentrated ammonia solution (28%) was added into the above mixture, and stirred for another 2 h. The product was washed with water and ethanol, and dried for 12 h.

1.3 Fabrication of CoSe-SC@NC, CoSe-SC and CoSe@NC composites.

The obtained Co-MOF@MPDA (Co-MOF, Co-NTAC@MPDA) was heated in a tubular furnace at 800 °C for 1 h under Ar atmosphere with a heating rate of 3 °C min^{-1}. Subsequently, well-ground selenium powder and Co-SC@NC (Co-SC, Co@NC) (in weight ratio 2:1) were placed in opposite corners of ceramic boat and placed in the upstream and middle side of the tubular furnace. The selenization was carried out at 450 °C for 3 h under H_2/Ar (5 vol % H_2) environment with 3 °C min^{-1} ramping rate. Finally, the CoSe-SC@NC (Co-SC, Co@NC) powder was naturally cooled to room temperature.

1.4 Preparation of $Na_3V_2(PO_4)_2O_2F$ cathode.

$Na_3V_2(PO_4)_2O_2F$ (NVPOF) was prepared via a simple hydrothermal method. Typically, A certain stoichiometric ratio of V_2O_5 and $H_2C_2O_4$ were firstly dissolved in the distilled water under stirring at 70 °C. Then, stoichiometric $NH_4H_2PO_4$ and NaF were added into the above solution under continuous stirring. Desired amount of $NH_3{\cdot}H_2O$ was added to adjust pH to neutral. After that, it was transferred into a Teflon-lined autoclave and kept at 170 °C for 12

hours. After natural cooling to room temperature, the jade-green NVPOF was rinsed with distilled water for several times, followed by drying in a vacuum oven for overnight.

2. Materials Characterization

The crystal structures of the samples were collected from a Bruker D8 Advance Powder XRD using Cu Kα radiation (λ = 0.15405 nm). The morphology of the materials was investigated using scanning electron microscopy (SEM, Philips XL30) and high resolution transmission electron microscopy (HRTEM, Tecnai G2) operating at 200 kV. Raman spectra were performed on a Renishaw Raman system model 2000 spectrometer using a 514.5 nm argon ion laser and calibrating referenced to the 520 cm^{-1} line of silicon. The surface chemical composition was analyzed by X-ray photoelectron spectrometry (XPS, ESCALAB MKII X-ray photoelectron spectrometer). BET surface area measurements were carried out by N_2 adsorption at 77.35 K on an Autosorbi Q Station 2. The CoSe content was characterized on Thermogravimetric Analyzer (TGA 4000, USA) in the presence of air with a heating rate of 10 °C min^{-1} under the temperature from 20 to 800 ℃.

3. Electrochemical Measurements

The anode slurry was prepared by mixing active materials, acetylene black (CB) and sodium carboxymethyl cellulose (CMC) binder with a weight ratio of 70:20:10 in water and then was coated on Cu foil followed by drying at 60 °C for 12 h in a vacuum oven. The mass loadings of the active materials were about 1 mg cm^{-2}. The electrolyte for SIBs is 3.0 M $NaPF_6$ in a mixed solvent of diethylene glycol dimethyl ether (DEGDME) and 1,3-dioxolane (DOL) in half cell. CR2032 coin-type cells were assembled in an Ar-filled glovebox (Mikrouna Universal 2440/750), in which H_2O and O_2 contents were less than 0.01 ppm. Glass fiber filter (Whatman GF/D) was used as the separator, while sodium foil serves as the counter electrode. The galvanostatic discharge/charge performance of batteries was tested on a Land battery testing system in the voltage window of 0.01-3 V vs. Na^+/Na for SIBs. Electrochemical impedance spectroscopy (EIS) tests were performed on a Solartron 1255 B frequency response analyzer from 100 kHz to 10 mHz with an applied amplitude of 10 mV amplitude voltage. CV tests were carried out using CHI 660E electrochemical workstation in the voltage range of 0.01-3 V at various scan rates (from 0.1 to 1.0 mV s^{-1}). For galvanostatic intermittent titration technique (GITT) analyses, the cells were cycled in the potential window of 0.01-3.0 V vs. Na^+/Na at a current density of 5 mA g^{-1}. The pulse time for each applied galvanostatic current and rest was 1 h and 6 h, respectively. All experiments were conducted at room temperature. The CoSe-SC@NC//NVPOF pouch full cells were assembled with CoSe-SC@NC as anode and NVPOF as cathode in an Ar-filled glove box. The separator and electrolyte performed in the full cells

were the same as in the half cells. The galvanostatic discharge/charge performance of full cells was tested on a Land battery testing system in the voltage window of 1.1-4.3 V.

4. Calculation Process for the Na^+ Diffusion Coefficients

The diffusion coefficients (D_{app}, Na) in CoSe-SC@NC and CoSe@SC electrodes are calculated from the galvanostatic intermittent titration technique (GITT) potential profiles by the following Weppner and Huggins equation,

$$D_{app,Na} = \frac{4}{\pi\tau}\left(\frac{m_B V_M}{M_B S}\right)^2\left(\frac{\Delta E_s}{\Delta E_\tau}\right)^2 (\tau << L^2/D)$$

Where m_B, M_B, and V_M are the mass, molecular weight, and molar volume of the as-prepared material, respectively; τ is the time for an applied galvanostatic current; S is the active surface of the electrode; L is the average radius of the material particles; and ΔE_s and ΔE_τ are the quasi-equilibrium potential and the change of cell voltage E during the current pulse, respectively.

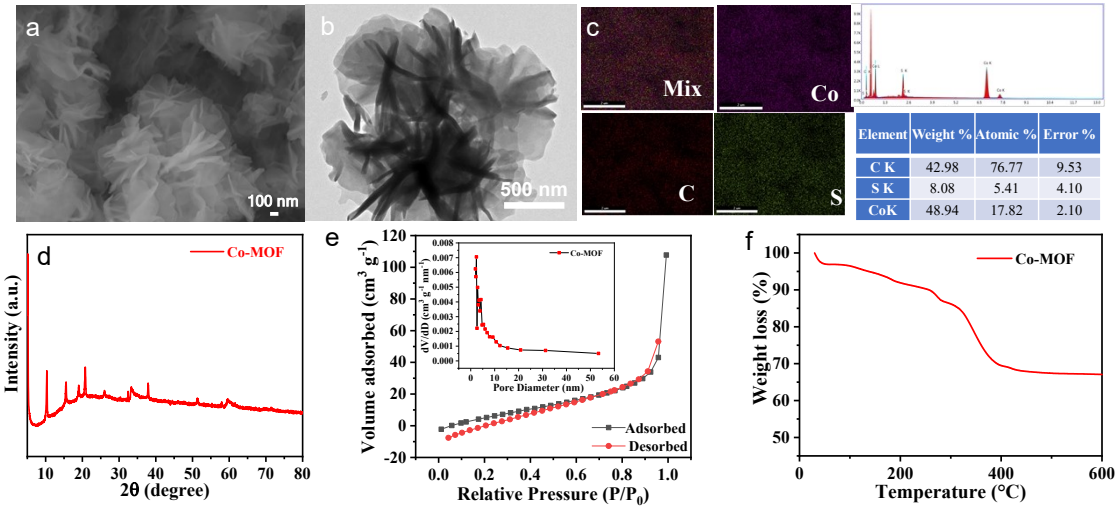

Fig. S1. Structural and compositional characterizations of Co-MOF. (a) SEM image. (b) TEM image. (c) Element Mapping. (d) XRD. (e) BET and corresponding pore size. (f) TGA curve.

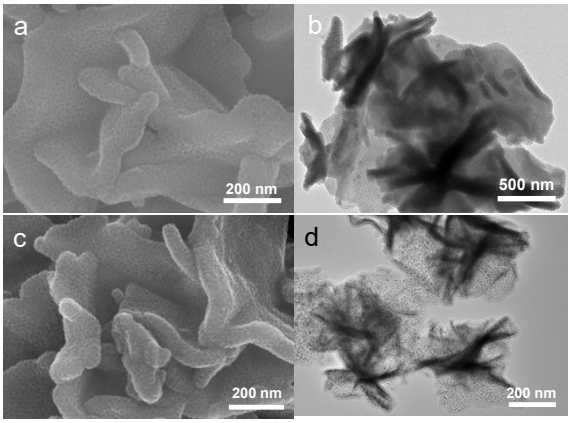

Fig. S2. SEM images (a, c) and TEM images (b, d) of Co-MOF@MPDA and Co-SC@NC.

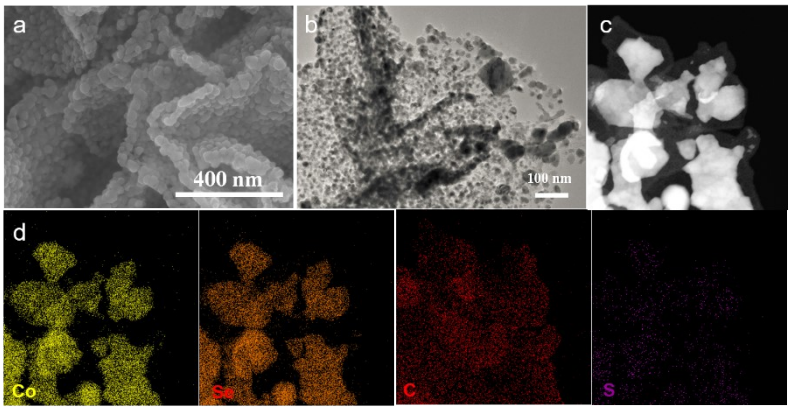

Fig. S3. (a, b) SEM images of CoSe-SC. (c) TEM and corresponding Co, Se, C, and S element mapping images of CoSe-SC.

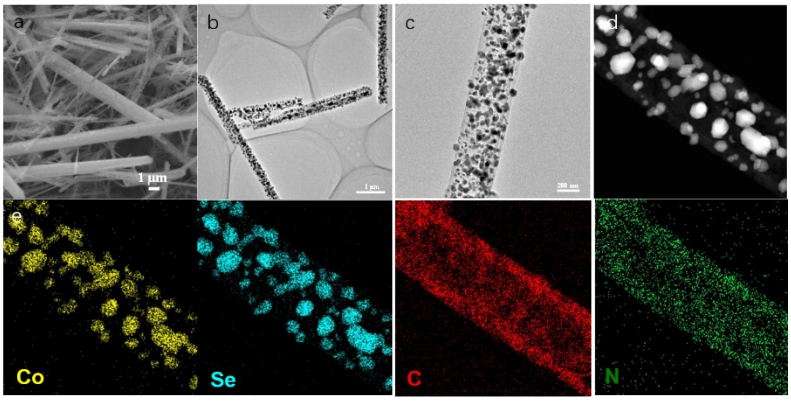

Fig. S4. (a-c) SEM images of CoSe@NC. (d, e) TEM and corresponding Co, Se, C, and N element mapping images of CoSe@NC.

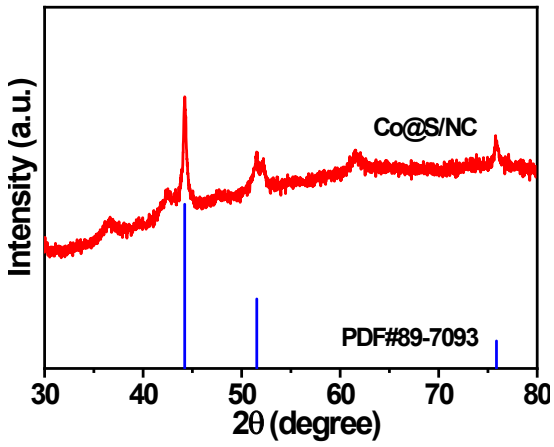

Fig. S5. XRD pattern of Co-SC@NC.

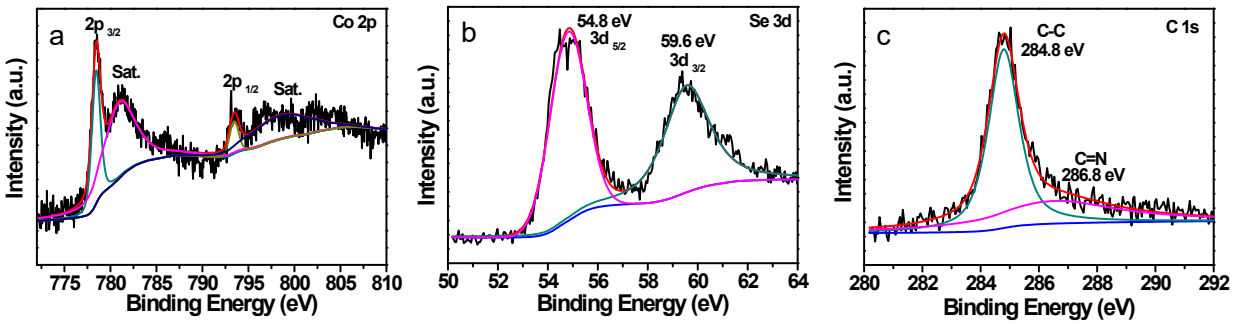

Fig. S6. High-resolution XPS spectra of CoSe-SC@NC: (a) Co 2p, (b) Se 3d, (c) C 1s.

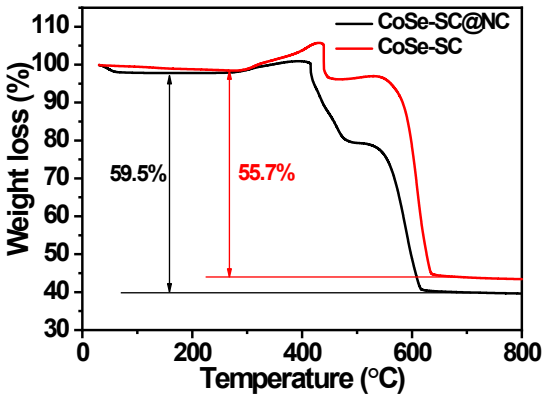

Fig. S7. The TGA curves of CoSe-SC@NC and CoSe-SC.

The detailed calculation process of the CoSe contents both in CoSe-SC@NC and CoSe-SC based on the TGA curves. According to the previous report[1], when the as-prepared samples (CoSe-SC@NC and CoSe-SC) were calcined in air, carbon was burned out, and the CoSe transformed into Co_3O_4. The CoSe content in as-prepared samples was calculated based on the following reactions:

$C(s) + O_2(g) = CO_2\ (g)$

$3CoSe(s) + 2O_2(g) = Co_3O_4(s) + 3Se(g)$

The CoSe content in CoSe-SC@NC is $3\times(M_{CoSe}/M_{Co3O4})\times(1-59.5\%) = 69.6\%$, and the CoSe content in bare CoSe-SC is $3\times(M_{CoSe}/M_{Co3O4})\times(1-55.7\%) = 76.1\%$.

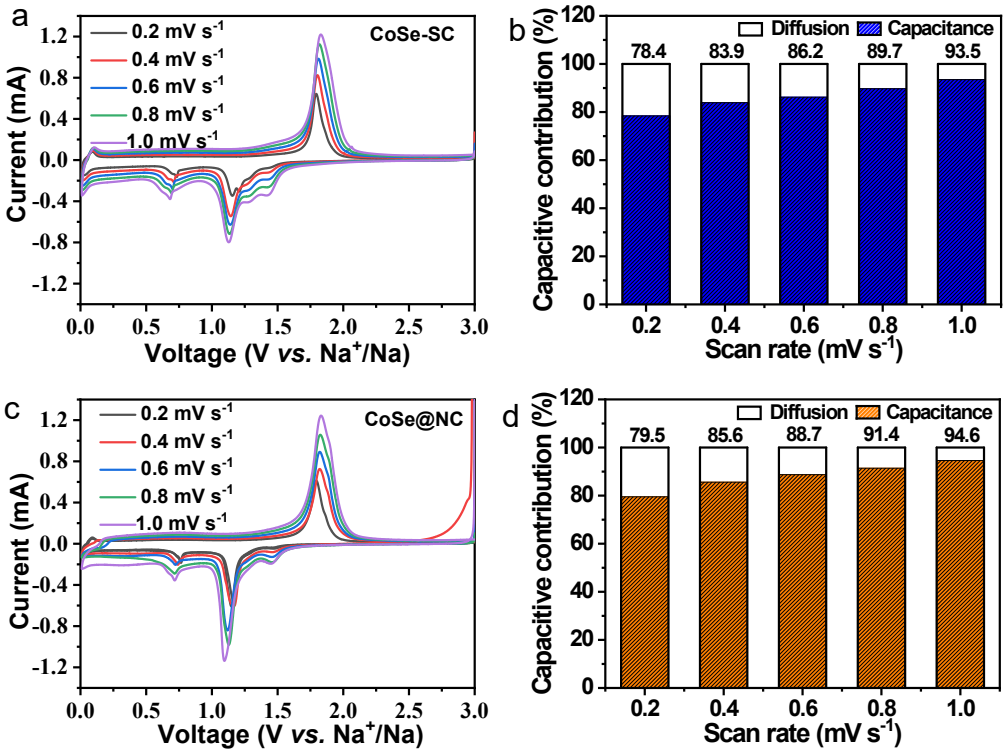

Fig. S8. Pseudocapacitive behavior of CoSe-SC and CoSe@NC.

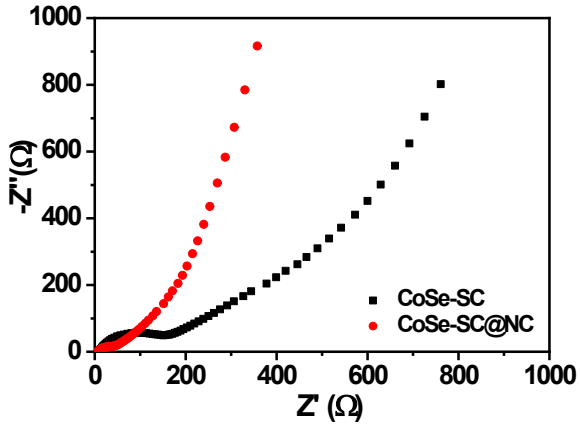

Fig. S9. EIS curves of CoSe-SC@NC and CoSe-SC.

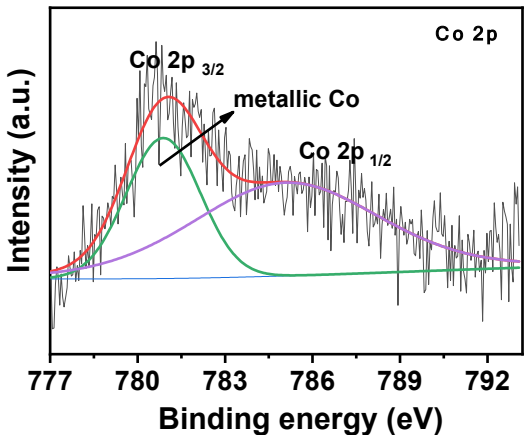

Fig. S10. XPS spectrum of Co 2p of CoSe-SC@NC electrode discharged to 0.01V.

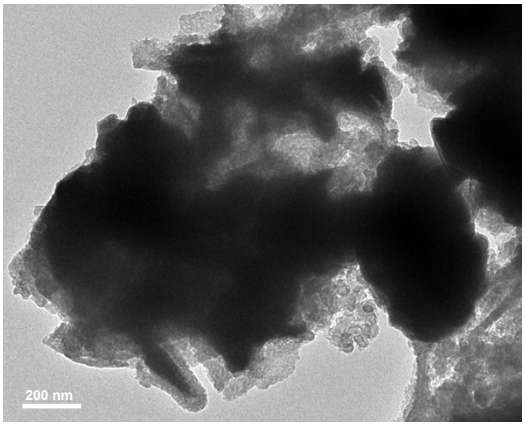

Fig. S11. TEM image of CoSe-SC@NC after 3 cycles.

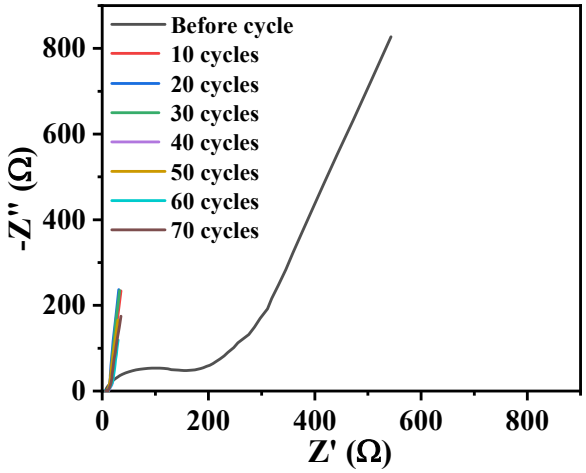

Fig. S12. EIS of CoSe-SC@NC electrode with different cycles.

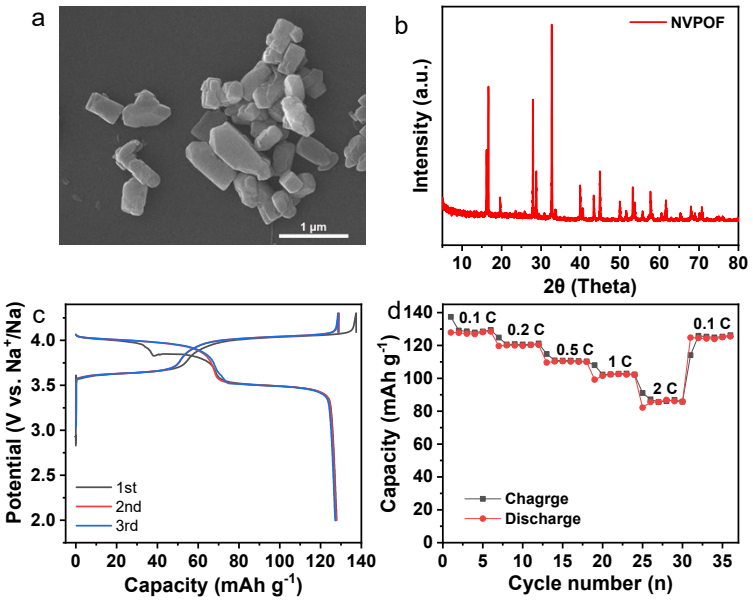

Fig. S13. (a) SEM image of $Na_3V_2O_2(PO_4)_2F$. (b) XRD pattern of $Na_3V_2O_2(PO_4)_2F$. (c) The initial charge-discharge voltage profiles for three cycles at 0.1 C rate. (d) Rate capability.

Table S1. Comparison of the electrochemical performances of cobalt selenide-based anode materials for SIBs.

Anode Materials	Current density ($A\ g^{-1}$)	Capacity ($mAh\ g^{-1}$)	References
CoSe-SC@NC	**5**	**419.7**	**This work**
$CoSe_2$@BCN-750	2	338	2
$CoSe_2$@C∩NC	2	300	3
$CoSe_2$/ZnSe	2	340	4
CoSe⊂carbon NWs	2	268	5
CoSe@PCP	2	282	6
CoSe@C	0.5	315	7
ZnSe/CoSe@NPC	2	318	8
P-$CoSe_2$	2	251.7	9

References

1 Y. Jiang; M. Xie; F. Wu; Z. Ye; Y. Zhang; Z. Wang; Y. Zhou; L. Li; R. Chen, *Small* **2021**, 2102893.

2 H. Tabassum; C. Zhi; T. Hussain; T. Qiu; W. Aftab; R. Zou, *Adv. Energy Mater.* **2019,** 9, 1901778.

3 B. Li; Y. Liu; X. Jin; S. Jiao; G. Wang; B. Peng; S. Zeng; L. Shi; J. Li; G. Zhang, *Small* **2019,** 15, 1902881.

4 G. Fang; Q. Wang; J. Zhou; Y. Lei; Z. Chen; Z. Wang; A. Pan; S. Liang, *ACS Nano* **2019,** 13, 5635.

5 C. Wu; Y. Jiang; P. Kopold; P. A. van Aken; J. Maier; Y. Yu, *Adv. Mater.* **2016,** 28, 7276.

6 J. Li; D. Yan; T. Lu; Y. Yao; L. Pan, *Chem. Eng. J.* **2017,** 325, 14.

7 M. Wang; H. Guo; C. An; Y. Zhang; W. Li; Z. Zhang; G. Liu; Y. Liu; Y. Wang, *J. Alloy. Compd.* **2020,** 820, 153090.

8 M. Jia; Y. Jin; C. Zhao; P. Zhao; M. Jia, *Appl. Surface Sci.* **2020,** 518, 146259.

9 J. Ye; X. Li; G. Xia; G. Gong; Z. Zheng; C. Chen; C. Hu, *J. Mater. Sci. Technol.* **2021,** 77, 100.